Physical analysis of an anisotropic eddy-viscosity concept for strongly detached turbulent unsteady flows

Rémi BOURGUET[1], Marianna BRAZA, Rodolphe PERRIN, Gilles HARRAN

Institut de Mécanique des Fluides de Toulouse, UMR 5502 CNRS-INPT/UPS, Allée du Prof. Camille Soula, 31400 Toulouse, France

[1] *Remi.Bourguet@imft.fr*

Abstract. A tensorial eddy-viscosity turbulence model is developed in order to take into account of the structural anisotropy appearing between the mean strain-rate tensor and the Reynolds turbulent stresses in strongly detached high Reynolds number flows. In the framework of the *Organised Eddy Simulation*, a physical investigation of the misalignment of these two tensor principal directions is performed by means of phase-averaged 3C-PIV measurements in the near-wake of a circular cylinder at Reynolds number 1.4×10^5. Considering the stress-strain misalignment as a local sign of the turbulence non-equilibrium, anisotropic criteria are derived. This leads to a tensorial eddy-viscosity concept which is introduced in the turbulent stress constitutive law. Additional transport equations for the misalignment criteria are derived from a degenerated SSG second order closure scheme. A two-dimensional version of the present model is implemented in the NSMB solver on the basis of a two-equation $k-\varepsilon$ isotropic OES model. Numerical simulation results are compared to an experimental dataset concerning the incompressible flow past a NACA0012 airfoil at 20^o degrees of incidence and Reynolds number 10^5.

Key words: Turbulence modeling, advanced URANS methods, Anisotropic *Organised Eddy Simulation*.

1. Introduction

In the context of high-Reynolds number turbulence modeling and especially in the case of parietal flows, recent advances like Large Eddy Simulation (LES) and hybrid methods (Detached Eddy Simulation, DES) have considerably improved the physical relevance of the numerical simulation. However, the LES approach is still limited to the low Reynolds number range concerning wall flows and the Unsteady Reynolds Averaged Navier-Stokes (URANS) approach remains a widespread and robust methodology for complex flow computation particularly in the near-wall region. Second-order closure schemes (Differential Reynolds Stress Modeling, DRSM) can provide an efficient simulation of turbulent stresses. Nonetheless, from a computational point of view, the main drawbacks of such approaches are a higher cost for unsteady and three-dimensional configurations and above all, numerical instabilities which imply the addition artificial dissipation terms. The present study is founded on the Organised Eddy Simulation (OES) methodology [1][2][3] which consists in distinguishing the flow structures to model according to their coherent or chaotic aspect instead of their size as in LES. The improvment of the advanced first order statistical approaches in the context of OES, especially in the sense of a realistic

simulation of the anisotropy tensor for non-equilibrium flows, represents one of the main objectives of the present development.
Concerning the first order statistical turbulence modeling, the linear eddy-viscosity models utilise the Boussinesq approximation [4] which establishes a linear relation between the Reynolds stresses and the strain-rate by means of a scalar eddy-viscosity concept. The Boussinesq law can be written as follows under the incompressibility assumption:

$$-\frac{\overline{u_i u_j}}{k} + \frac{2}{3}\delta_{ij} = -a_{ij} = 2\frac{\nu_t}{k}S_{ij},$$

where $\overline{u_i u_i}$ are the turbulent stresses, k is the turbulent kinetic energy ($k = \frac{1}{2}\overline{u_i u_i}$), δ_{ij} is Kronecker symbol and S the mean strain-rate tensor, defined by $S_{ij} = \frac{1}{2}\left(\frac{\partial U_i}{\partial x_j} + \frac{\partial U_j}{\partial x_i}\right)$. U_i is the mean flow velocity. ν_t is the scalar eddy-viscosity that is often expressed by means of the turbulence length and time scales as $\nu_t = C_\mu k^2/\varepsilon$, where ε is turbulence dissipation rate.
The Boussinesq approximation assumes, among others, that the principal directions of the two tensors $-a$ and S always remain collinear. This leads to an overproduction of turbulent kinetic energy [5] especially in flow regions upstream of the detachment, where the strain-rate is high and the flow is laminar [6][7].
The Non-Linear Eddy-Viscosity Models (NLEVM) provides modified behaviour laws which attempt to overcome these limitations. The associated constitutive laws are derived from a complete tensorial basis of the turbulent stresses [8][9] involving quadratic or cubic combinations of the strain and vorticity tensors. The Explicit Algebraic Stress Models which are derived from algebraic forms of the turbulent stresses issued from the DRSM [10][11][12][13] provide improved results for non-equilibrium flows but imply significant calibration processes according to the flow configuration of interest [14][15].
In the framework of OES methods, an alternative to NLEVM is suggested to derive a tensorial eddy-viscosity model sensitised for non-equilibrium turbulence [16]. As discussed in the present paper, the non-equilibrium can be illustrated by means of stress-strain misalignment [17], among other concepts, as well as by the ratio of the mean flow time-scale over the turbulence time-scale [11]. A selective reduction of the eddy-diffusion coefficient, varying according to the non-equilibrium flow regions and the coherent flow structures, to reach an improved prediction of the turbulence production in respect of the flow physics, is expected. As presented in the first section, the analysis of the stress-strain behaviour is based on a detailed high-Reynolds PIV experiment concerning the incompressible flow past a circular cylinder at Reynolds number 1.4×10^5 in high blockage and aspect ratios [18]. The phase-averaged turbulence properties are considered, allowing distinction of the organised coherent physical process from the random turbulence. Furthermore, anisotropic misalignment criteria are investigated and a tensorial definition of the eddy-viscosity is put forward, leading to a new Reynolds stress constitutive law. Transport equations for these criteria are derived from the Speziale, Sarkar and Gatski second order closure scheme [19]. The predictive capacities of this anisotropy resolving approach are examined in the last section by comparison of two-dimensional numerical simulation results issued from NSMB solver with an experimental dataset concerning the incompressible flow around a NACA0012 airfoil at 20^o degrees of incidence and Reynolds number 10^5.

2. Stress-strain anisotropy as a non-equilibrium criterion

2.1. The Organised Eddy Simulation framework

The OES methodology consists in a separation of the turbulent kinetic energy spectrum into a resolved part corresponding to organised flow structures and a modeled part associated with chaotic fluctuations. Experimental studies emphasised a modification the spectrum to be modeled in the inertial region where coherent structures and random turbulence interact [2][3]. This modification, which illustrates the non-equilibrium compared to the equilibrium turbulence described by Kolmogorov's statistical theory, implies a recalibration of the turbulence time and lengh scales in URANS methodology. The OES approach proposed a modification of the diffusivity constant C_μ in two-equation closure schemes, using an isotropic Boussinesq law as a first step, and this methodology reached an efficient prediction of massively detached unsteady turbulent flows around bodies. From a physical point of view, a consequence of the non-equilibrium is the misalignment observed between the Reynolds stress and mean strain-rate tensor. In the present study, the structural properties of this misalignment are used to reach a more relevant prediction of the non-equilibrium turbulence physics.

2.2. An investigation of the stress-strain misalignment via 3C-PIV in the cylinder wake

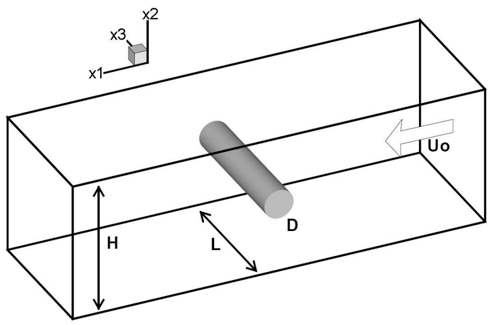

Figure 1. Flow configuration.

The experiment has been carried out in the wind tunnel S1 of IMFT. The channel has a $670 \times 670\text{mm}^2$ cross section. The cylinder spans the width of the channel without endplates and has a diameter D of 140mm, giving an aspect ratio $L/D = 4.8$ and a blockage coefficient $D/H = 0.208$. The upstream velocity U_0 at the centre of the channel is 15m/s, therefore the Reynolds number based on the upstream velocity and the cylinder diameter D is 1.4×10^5. The free stream turbulence intensity, measured by hot wire technique in the inlet was found 1.5%. The three-component measurements have been performed by means of stereoscopic PIV. The procedure used is reported in [18]. In the present study, the median plan has been considered at half distance spanwise and located in the near-wake region (Fig. 1).

The near periodic nature of the flow, due to the von Kármán vortices, allows the definition of a phase. In the following all quantities are phase-averaged. Angles between the principal directions of the strain-rate and turbulence anisotropy tensors are quantified. The main coherent vortex regions are delimited by the Q criterion [20]. The first principal directions of each tensor are represented in Fig. 2. In specific flow regions their misalignment becomes predominant. The largest misalignment is observed near the vortex center ($x_1/D = 1$, $x_2/D = 0.03$) in Fig. 2(a) for instance. The best alignment is reached in free shear flow regions.

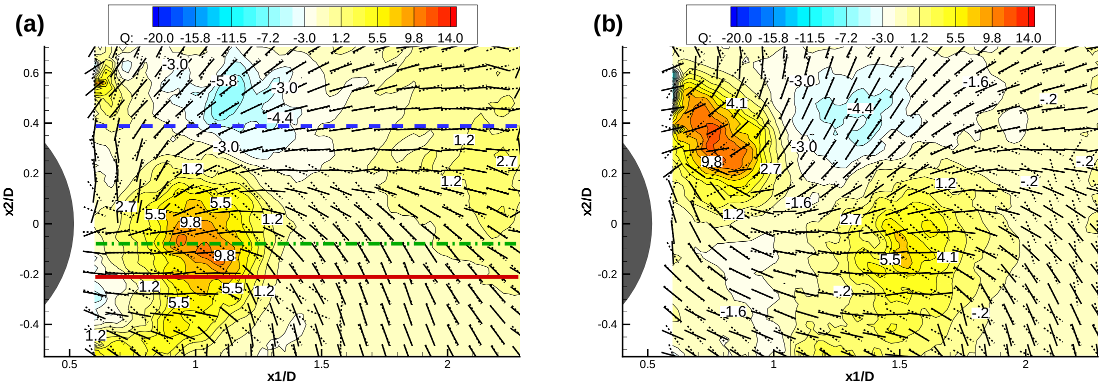

Figure 2. $-a$ *(dashed) and* S *(solid) first principal directions and* Q *criterion iso-contours at phases (a)* $\varphi = 50^o$ *and (b)* $\varphi = 140^o$.

In Fig. 3 the angle between the directions of v_1^a and v_1^S is represented for given ordinates (cf. bold lines in Fig. 2(a)). In spite of the measurement noise induced by PIV technic, the solid and dashed-dotted curves ($x_2/D = -0.21$ and $x_2/D = -0.06$, respectively) confirm the misalignment peak near the vortex center (up to 50^o around $x_1/D = 1$) whereas the dashed curve ($x_2/D = 0.39$) demonstrates a quasi-alignment near the saddle point and in free flow regions (beyond $x_1/D = 1.5$).

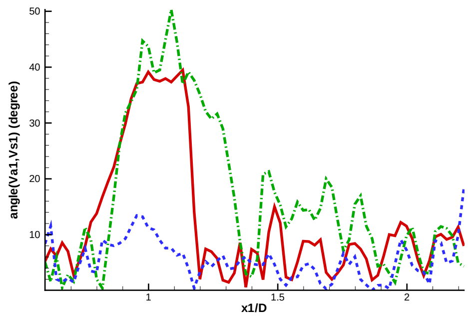

Figure 3. Angle variation between $-a$ *and* S *first principal directions along the three lines in bold in Fig. 2(a).*

2.3. An anisotropic misalignment criterion

The analysis of the high misalignment zones allows to locate precisely the validity regions of the Boussinesq isotropic law. As a consequence, in the perspective of an improvment of the Reynolds tensor constitutive law, it seems judicious to take into account of these effects. However, a direct monitoring of the misalignment between the three principal directions of the two tensors implies an assumed knowledge about these tensors which does not make sense since the stress tensor is derived from the constitutive law. In this context, a misalignment criterion is defined as the correlation rate between the projection of the anisotropy tensor onto the eigen basis of the strain-rate tensor and the corresponding eigenvector of S. Without any estimation of the eigenvectors of $-a$, this directional criterion can provide sufficient information about the alignment between the principal directions of $-a$ and v_i^S, in each space direction:

$$C_i = -\frac{a_{jk}\left(v_i^S\right)_k\left(v_i^S\right)_j}{\|av_i^S\|} \quad \text{for} \quad i = 1, 2, 3, \quad \text{where } \|.\| \text{ is the euclidian norm.}$$

The C_i coefficients gives an anisotropic knowledge which enables to describe locally the distortion between the stress and strain-rate tensors, allowing a distinction between the global and planar misalignment as presented schematically in Fig. 4.

As can be shown in the present experiment, the criterion decreases in highly-strained shear flow regions and especially near the vortex center whereas it remains maximum when the two principal tensorial directions are aligned. Moreover, this directional criterion is "advectable" through specific transport equations that can be derived from DRSM as suggested in the next section.

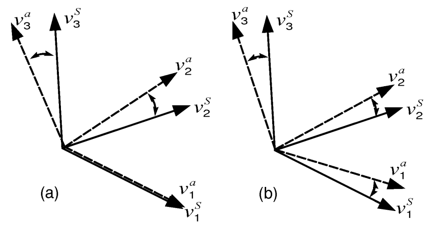

Figure 4. *C_i anisotropic criterion discriminates (a) planar and (b) global misalignments.*

3. An anisotropic first order eddy-viscosity model

3.1. The tensorial eddy-viscosity concept

The previous analysis concerning the specific decorrelations between Reynolds stress and mean strain-rate tensors in each space direction demonstrates the relevance of a constitutive law taking account of the individual contribution of each element of a spectral decomposition which is applied to the strain-rate tensor. The following definition of an anisotropic eddy-diffusion coefficient can be suggested by an extension of the scalar C_μ definition, for $i = 1, 2, 3$:

$$C_{\mu_i} = \frac{\left| a_{jk} \left(v_i^S\right)_k \left(v_i^S\right)_j \right|}{\eta_i} = |C_{Vi}| \frac{\varepsilon}{k} \quad \text{where} \quad C_{Vi} = -\frac{a_{jk} \left(v_i^S\right)_k \left(v_i^S\right)_j}{|\lambda_i^S|}.$$

$\eta_i = \frac{k|\lambda_i^S|}{\varepsilon}$ is a vectorial version of $\eta = \frac{k\|S\|}{\varepsilon}$ mean flow/turbulent time scale rate which emphasises the non-equilibrium turbulence regions [11]. Whenever η is higher than 3.3 approximately, the non-equilibrium turbulence becomes predominant.

Therefore a consistent definition of the eddy-viscosity as a symmetric tensor ν_{tt} is suggested on the basis of a positive directional eddy-viscosity ν_{td} :

$$(\nu_{tt})_{ij} = (\nu_{td})_k \left(v_k^S\right)_i \left(v_k^S\right)_j \quad \text{with} \quad (\nu_{td})_i = |C_{Vi}|\, k. \tag{1}$$

Expression (1) leads to a weighted summation of S spectral decomposition:

$$S_{ik} (\nu_{tt})_{kj} = (\nu_{td})_l \, \lambda_l^S \left(v_l^S\right)_i \left(v_l^S\right)_j = (\nu_{td})_l \, (S_l)_{ij}\,, \tag{2}$$

and thus, the linear EVM behaviour law can be generalised as:

$$-\overline{u_i u_j} + \frac{2}{3} k\delta_{ij} = 2S_{ik} (\nu_{tt})_{kj} - \frac{2}{3} R\delta_{ij}, \tag{3}$$

where $R = (\nu_{td})_i \, \lambda_i^S$ is the trace of $S_{ik} (\nu_{tt})_{kj}$. From expression (2), the symmetry property of the turbulence anisotropy tensor is ensured. Expression (3) leads to the following generalization of averaged Navier-Stokes momentum equations:

$$\frac{DU_i}{Dt} = \frac{\partial}{\partial x_j} \left(\nu \left(\frac{\partial U_i}{\partial x_j} + \frac{\partial U_j}{\partial x_i} \right) + (\nu_{tt})_{kj} \left(\frac{\partial U_i}{\partial x_k} + \frac{\partial U_k}{\partial x_i} \right) - \frac{2}{3} (k + R)\, \delta_{ij} \right) - \frac{1}{\rho} \frac{\partial P}{\partial x_i}.$$

The tensorial definition enables a selective reduction of the effect of one (or more) elements of the strain-rate tensor spectral decomposition with respect to the corresponding physical alignment (or misalignment) between the associated principal directions. Moreover, if a perfect alignment is observed in an equilibrium and isotropic strain region the tensorial expression degenerates into a classical Boussinesq-like scalar model.

3.2. "Experimental" validation

Comparison between normal and shear Reynolds stresses evaluated from the PIV experiment and from modelling via (3) and measured stress tensor at two location points and over a period of vortex shedding is presented in Fig. 5 and can be regarded as an "experimental" validation. The modelled quantities present a good match with the experiment for both normal and shear Reynolds stresses. This is verified when examining the complete fields at a given phase angle (Fig. 6): despite slight differences in shear flow region, the predictive capacities of the tensorial constitutive law are confirmed.

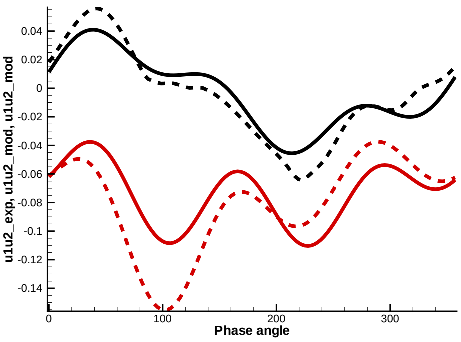

Figure 5. *Comparison between measured (solid) and modeled (dashed) Reynolds stresses: shear layer (red) and wake (black).*

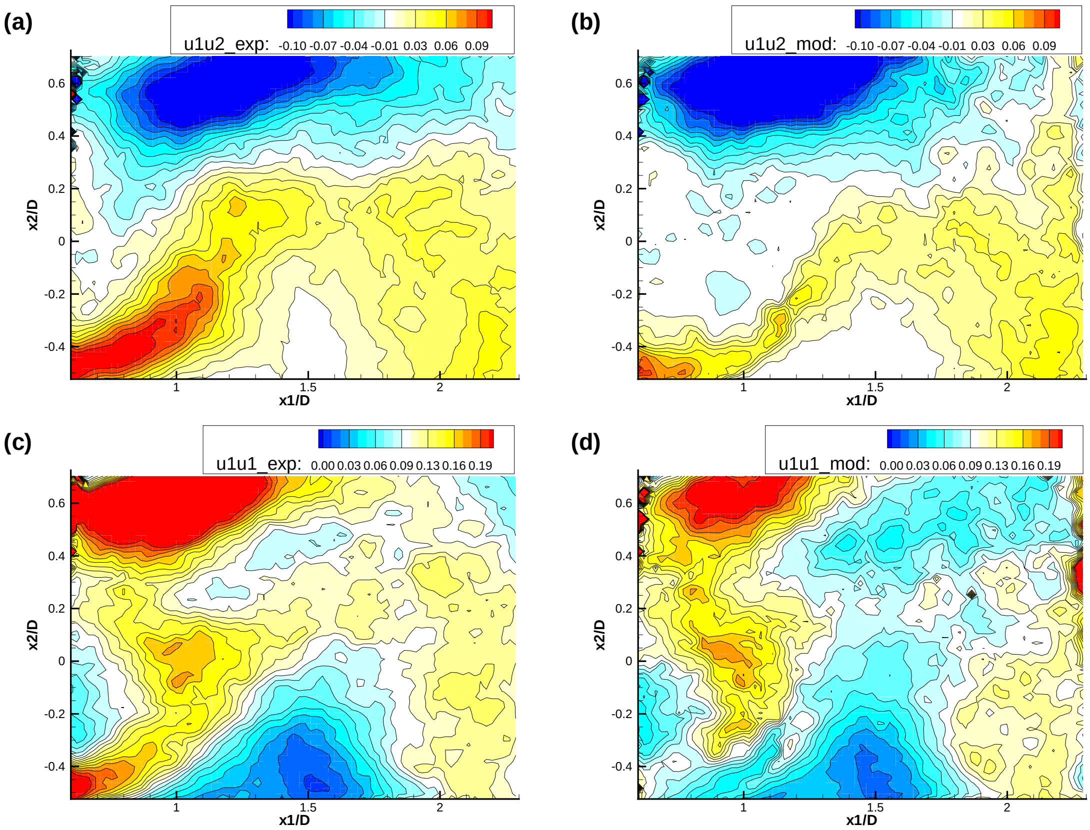

Figure 6. *Comparison between phase-averaged Reynolds stresses $\overline{u_i u_j}$ obtained directly from the PIV experiment (a) shear and (c) normal, and those evaluated via equation (3) and experimental strain-rate tensor (b) shear and (d) normal at phase $\varphi = 50^o$.*

3.3. An anisotropic first order closure scheme

From a degeneration of the Speziale, Sarkar and Gatski second order closure scheme [19], three advection equations are derived to transport the C_{Vi} coefficients as state variables of the physical system. For $q = 1, 2, 3$:

$$\frac{DC_{Vq}}{Dt} = -\frac{1}{\left|\lambda_q^S\right|}\left((V_q)_{ij}\frac{Da_{ij}}{Dt} + a_{ij}\frac{D\,(V_q)_{ij}}{Dt} + C_{Vq}\frac{D\left|\lambda_q^S\right|}{Dt} \right) \text{ with } (V_q)_{ij} = \left(v_q^S\right)_i\left(v_q^S\right)_j,$$

which leads by introducing the SSG modeling for the pressure/strain correlation in a similar way as [21] for a non-directional misalignment:

$$\begin{aligned} \frac{DC_{Vq}}{Dt} &= \left(\frac{4}{3} + c_3^* II_a^{\frac{1}{2}} - c_3\right)\frac{(V_q)_{ij}S_{ij}}{\left|\lambda_q^S\right|} + (2-2c_4)\frac{(V_q)_{ij}\,a_{ik}S_{jk}}{\left|\lambda_q^S\right|} - \frac{c_2}{\eta_q}(V_q)_{ij}a_{ik}a_{kj} \\ &+ (2-2c_5)\frac{(V_q)_{ij}a_{ik}\Omega_{jk}}{\left|\lambda_q^S\right|} + (1-c_1)\frac{\varepsilon}{k}C_{Vq} + (1+c_1^*)\,C_{Vq}a_{ij}S_{ij} + \frac{c_2 II_a}{3\eta_q} \\ &+ \frac{2\,(c_4-1)}{3}\frac{a_{ij}S_{ij}}{\left|\lambda_q^S\right|} - \frac{1}{\left|\lambda_q^S\right|}\left(a_{ij}\frac{D\,(V_q)_{ij}}{Dt} + C_{Vq}\frac{D\left|\lambda_q^S\right|}{Dt}\right) + D^{C_{Vq}} \end{aligned}$$

where $D^{C_{Vq}}$, the diffusion term can be approximated by:

$$D^{C_{Vq}} = \frac{\partial}{\partial x_i}\left(\left(\nu + \frac{(\nu_{tt})_{ij}}{\sigma_{C_{Vq}}}\right)\frac{\partial C_{Vq}}{\partial x_j}\right).$$

$II_a = a_{ij}a_{ij}$, and the seven constants c_i and c_i^* are reported in Tab. 1.

Table 1. SSG second order closure scheme constants [19].

c_1	c_1^*	c_2	c_3	c_3^*	c_4	c_5
1.7	0.90	1.05	0.8	0.65	0.625	0.2

Assuming a similarity with the diffusion term of k transport equation, $\sigma_{C_{Vq}}$ coefficient can be set, firstly, to the value of one.

4. Numerical results

4.1. Implementation in the Navier-Stokes Multi-Block solver

On the basis of the $k-\varepsilon$ OES turbulence model, the previous transport equations were implemented in the Navier-Stokes Multi-Block (NSMB) code. The NSMB solver is constructed on a finite volume formulation of the fully compressible Navier-Stokes governing equations. In the present study, spatial discretization is ensured by a second order central scheme and temporal intergration by a second order backward scheme based on a dual time stepping method with constant CFL parameters. More details about NSMB numerical issues can be found in [22] and validation results concerning the C type meshgrid (256×81 nodes) used in the present configuration are reported in [23].

The isotropic OES version of the $k - \varepsilon$ two-equation closure scheme is founded on Chien's low Reynolds number model [24] where eddy-diffusivity coefficient and damping function were reconsidered to take into account of the turbulent kinetic energy spectrum modification induced by the extraction of phase-avared quantities in non-equilibrium turbulent configurations. In the present development, the scalar C_μ parameter is replaced by the tensorial one and the following isotropic OES damping function is considered, leading to a reduction of the eddy-viscosity closer to the wall than using Chien's function:

$$f_\mu \left(y^+\right) = 1 - \exp\left(-0.0002\, y^+ - 0.000065\, y^{+2}\right),$$

where y^+ is the non-dimensional wall distance.

4.2. Detached turbulent flow around a NACA0012 airfoil

The predictive capacities of the present anisotropic turbulence model are analysed on a well-documented two-dimensional test-case, at first. The incompressible unsteady flow past au NACA0012 airfoil at 20^o degrees of incidence is simulated by means of the present model. The Reynolds number based on the chord length and the free-stream velocity is equal to 10^5. The numerical results are compared to an experimental dataset [25]. As presented in Fig. 7, the C_{Vi} criteria transported by the additional equations allow a local modulation of the eddy-diffusion coefficient, leading to specific reductions in highly sheared region and in the near-wake coherent structures. In the far-wake where a certain equilibrium is reached, a homogenisation of the criterion is observed.

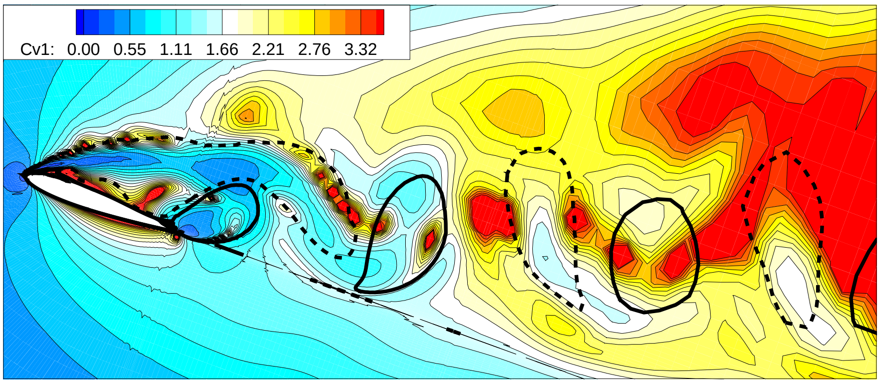

Figure 7. Iso-contours of the first misalignment criterion C_{V1} and iso-lines of the vorticity $\omega_y = 0.25$ (bold solid lines) and $\omega_y = -0.25$ (bold dashed lines), NACA0012 airfoil at 20^o degrees of incidence $R_e = 10^5$ and $M = 0.18$ (NSMB simulation).

A comparison between the experimental and computed aerodynamic efforts emphasises the quality of the anisotropic turbulence model in this two-dimensionnal context (Fig. 8). Numerical values are slightly higher than the experimental ones. Relative errors are $< 2.5\%$ for the lift coefficient ($C_z = 0.771/0.753$) and $< 2\%$ for the drag coefficient ($C_x = 0.325/0.320$), which demonstrates the capacity of the present approach to predict with a high physical reliability this strongly detached turbulent flow.

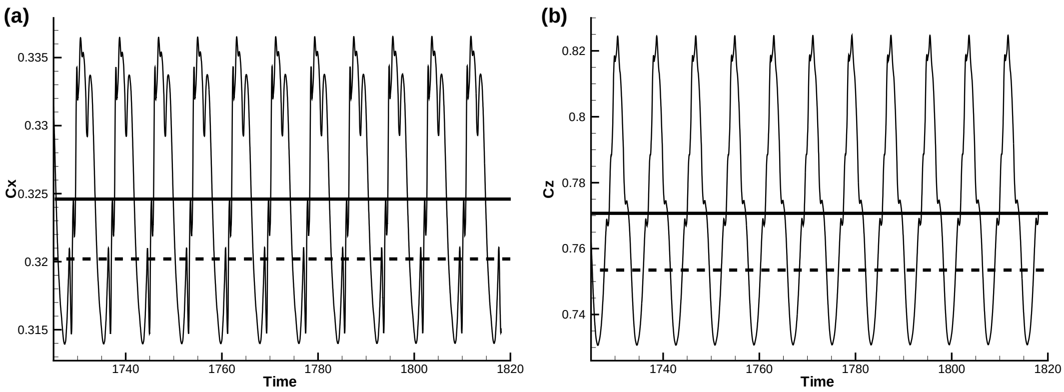

Figure 8. (a) drag and (b) lift coefficients computed by means of the present anisotropic model (solid curve), time-averaged simulation values (bold solid line) and experimental results (dahsed line).

5. Conclusion

In the present study, the misalignment between the phase-averaged turbulent stresses and the strain-rate tensor has been quantified in the regions of the coherent vortices and in the highly sheared ones downstream of the separation. This physical investigation was performed on the basis of a phase-averaged 3C-PIV experiment which allowed accessing detailed fields of turbulence quantities relevant to the flow physics. A directional criterion was defined in order to monitor the anisotropy of the two tensors in each space direction. This yielded an anisotropic tensorial eddy-viscosity concept sensitised in respect of the non-equilibrium turbulence. A significant match was achieved between the modelled turbulence stresses and the experimental ones under the phase-averaged decomposition. Furthermore, in the perspective of numerical implementations, advection equations were derived from the SSG second order closure scheme [19] in order to transport the anisotropic misalignment criterion as new state variables. The two-dimensional version of this tensorial first order model was validated on a relevant test-case and the comparison of the simulated global aerodynamic coefficients to experimental datas emphasises the promising predictive capacity of this turbulence modeling approach.

Acknowledgments

The numerical implementation was performed in collaboration with Dr. J.B. Vos (Computational Fluid and Structure Engineering, CFSE and Ecole Polytechnique Fédérale de Lausanne, EPFL) and Dr. Y. Hoarau (Institut de Mécanique des Fluides et des Solides, IMFS de Strasbourg) who are gratefully acknowledged. The calculations were performed at the Centre Informatique National de l'Enseignement Supérieur (CINES), the Institut du Développement et des Ressources en Informatique Scientifique (IDRIS) and the Centre Interuniversitaire de Calcul de Toulouse (CICT). The first author was financially supported by the Centre National de la Recherche Scientifique (CNRS) and the Délégation Générale pour l'Armement (DGA).

References

[1] A. BOUHADJI, S. BOURDET, M. BRAZA, Y. HOARAU, P. RODES and G. TZABIRAS. *Turbulence modelling of unsteady flows with a pronounced periodic character.* Notes on Numerical Fluid Mechanics and Multidisciplinary Design, 81:87-96, Springer, 2002.

[2] M. BRAZA, R. PERRIN and Y. HOARAU. *Turbulence Properties in the cylinder wake at high Reynolds number.* J. Fluids and Structures, 22:755-771, 2006.

[3] R. PERRIN, M. BRAZA, E. CID, S. CAZIN, A. SEVRAIN, M. STRELETS, M. SHUR, Y. HOARAU, A. BARTHET, G. HARRAN and F. MORADEI. *3D circular cylinder.* Notes on Numerical Fluid Mechanics and Multidisciplinary Design, 94:299-312, Springer, 2006.

[4] J. BOUSSINESQ. *Théorie de l'écoulement tourbillant.* Mém. prés. par div. Sav. à l'Acad. Sci., Paris, 23:46-50, 1877.

[5] P.S. KLEBANOFF. *Characteristics of Turbulence in a Boundary Layer with Zero Pressure Gradient.* NACA Technical Note, 3178, 1954.

[6] P.A. DURBIN and B.A. PETTERSSON REIF. *Statistical Theory and Modeling for Turbulent Flow.* John Wiley, 2001.

[7] G. JIN and M. BRAZA. *A two-equation turbulence model for unsteady separated flows around airfoils.* AIAA J. , 32(11):2316-2320, 1994.

[8] S.B. POPE. *A More General Effective-Viscosity Hypothesis.* J. Fluid Mech., 72:331340, 1975.

[9] T.B. SHIH, J. ZHU and J.L. LUMLEY. *A realizable Reynolds stress algebraic equation model.* NASA TM 105993, ICOMP-92-27, CMOTT-92-14, 1993.

[10] T. JONGEN and T.B. GATSKI. *General Explicit Algebraic Stress Relations and Best Approximation for Three-Dimensional Flows.* Int. J. Engr. Sci., 36:739-763, 1998.

[11] C.G. SPEZIALE and X.H. XU. *Towards the development of second-order closure models for non-equilibrium turbulent flows.* Int. J. Heat and Fluid Flow, 17:238-244, 1996.

[12] T.B. GATSKI and C.G. SPEZIALE. *On Explicit Algebraic Stress Models for Complex Turbulent Flows.* J. Fluid Mech., 254:5978, 1993.

[13] S. WALLIN and A.V. JOHANSSON. *An explicit algebraic Reynolds stress model for incompressible and compressible turbulent flows.* J. Fluid Mech., 403:89, 2000.

[14] W. HAASE, V. SELMIN and B. WINZELL. *Progress in Computational Flow-Structure Interaction.* Notes on Numerical Fluid Mechanics and Multidisciplinary Design, 81, Springer, 2002.

[15] W. HAASE, B. AUPOIX, U. BUNGE and D. SCHWAMBORN. *FLOMANIA- A European Initiative on Flow Physics Modelling.* Notes on Numerical Fluid Mechanics and Multidisciplinary Design, 94, Springer, 2006.

[16] R. BOURGUET, M. BRAZA, R. PERRIN and G. HARRAN. *Anisotropic eddy-viscosity concept for strongly detached unsteady flows.* AIAA J., in press, 2007.

[17] H.S. KANG and C. MENEVEAU. *Effect of large-scale coherent structures on subgrid-scale stress and strain-rate eigenvector alignments in turbulent shear flow.* Phys. Fluids, 17:055103, 2005.

[18] R. PERRIN, M. BRAZA, E. CID, S. CAZIN, F. MORADEI, A. BARTHET, A. SEVRAIN and Y. HOARAU. *Near-wake turbulence properties in the high Reynolds incompressible flow around a circular cylinder by 2C and 3C PIV.* 6^{th} ERCOFTAC International Symposium on Engineering Turbulence Modelling and Measurements - ETMM6, proceedings, 2005, J. Flow Turb. and Combust, in print.

[19] C.G. SPEZIALE, S. SARKAR and T.B. GATSKI. *Modeling the pressure strain correlation of turbulence: an invariant dynamical systems approach.* J. Fluid Mech., 227:245-272, 1991.

[20] J.C. HUNT, A. WRAY and P. MOIN. *Eddies, stream, and convergence zones in turbulent flows.* Center for Turbulence Research Report,CTR-S88, 1988.

[21] A.J. REVELL, S. BENHAMADOUCHE, T. CRAFT, D. LAURENCE and K. YAQOBI. *A stress-strain lag eddy viscosity model for unsteady mean flow.* Eng. Turb. Model. and Exp., 6:117-126, 2005.

[22] J.B. VOS, E. CHAPUT, B. ARLINGER, A. RIZZI et A. CORJON. *Recent advances in aerodynamics inside the NSMB (Navier-Stokes Multi-Block) consortium.* In 36th Aerospace Sciences Meeting and Exhibit, AIAA Paper 0802, Reno, USA, 1998.

[23] A. BOUHADJI, S. BOURDET, M. BRAZA, Y. HOARAU, P. RODES and G. TZABIRAS. *Turbulence modelling of unsteady with a pronounced periodic character.* Progress in Computational Flow-Structure Interaction, In Notes on Numerical Fluid Mechanics, 81:251-260, 2002.

[24] K.Y. CHIEN. *Predictions of Channel and Boundary-Layer Flows with a Low-Reynolds-Number Turbulence Model.* AIAA J., 20(1):33-38, 1982.

[25] E. BERTON, D. FAVIER et C. MARESCA. *Progress in Computational Flow-Structure Interaction.* Notes on Numerical Fluid Mechanics, 81, Springer, 2002.